Strength by Atomic Force Microscopy (A Kelly special issue)

Kevin Kendall, Aman Dhir, Chin Yong

Strength by Atomic Force Microscopy (A Kelly special issue)

Journal:	*Philosophical Magazine & Philosophical Magazine Letters*
Manuscript ID:	TPHM-09-Aug-0348.R1
Journal Selection:	Philosophical Magazine
Date Submitted by the Author:	10-Nov-2009
Complete List of Authors:	Kendall, Kevin; University of Birmingham, Chemical Engineering Dhir, Aman; University of Birmingham, Chemical Engineering Yong, Chin; Daresbury Lab, Computing
Keywords:	atomic force microscopy, fracture, indentation testing, molecular dynamic simulations
Keywords (user supplied):	

Strength by Atomic Force Microscopy (AFM): Molecular dynamics of water layer squeezing on magnesium oxide

K Kendall, Aman Dhir

Chemical Engineering, University of Birmingham

Chin Yong

STFC, Daresbury Laboratory

Warrington

Abstract

Localised strength testing of materials is often carried out in the Atomic Force Microscope (AFM) as foreseen by Kelly in his book Strong Solids. It is known that contamination during AFM indentation experiments can strongly influence the observed strength, but a major problem is the theoretical interpretation of the results. Here we use molecular dynamics computer modelling to describe the contact of NaCl and MgO crystal probes onto surfaces, comparable to an AFM experiment. Clean NaCl gave elastic, brittle behaviour in contact simulations at 300K whereas MgO was more plastic, leading to increased toughness. This paper goes on to consider the strength of an oxide substrate contaminated by water molecules tested by indentation with a pyramidal probe of oxide crystal. Recent theory on the effect of liquid contaminant layers on surface strength has been mainly focussed on Lennard Jones (LJ) molecules with some studies on alcohols and water, described by molecular dynamics, which allows the molecules to be squeezed out as the crystal lattice is deformed. In this work we have focused on water by studying the forces between a magnesium oxide (MgO) atomic force microscope (AFM) probe and an MgO slab. Force versus separation has been plotted as the AFM probed was moved towards and away from the substrate. Simulation results showed that the water layers could be removed in steps, giving up to four force peaks. The last monolayer of water could not be squeezed out even at pressures where MgO deformed plastically. Interestingly, with water present, the strength was reduced but more in tensile

than compressive measurements. In conclusion, water contaminating the oxide surface in AFM strength testing is structured. Water layer squeezing removal can be predicted by molecular modelling which may be verified by AFM experiments to show that water can influence the strength of perfect crystals at the nanometer scale.

Key words:- AFM; molecular dynamics model; MgO; water squeezing.

1. Introduction

In the book Strong Solids, Kelly and Macmillan [1] discussed the highest stress that could be withstood by a perfect material such as a single crystal of NaCl or MgO following the original calculations of Zwicky [2] and described the idea that a nanometre scale indenter would be likely to locate a region that was locally free of defects such as cracks or dislocations, leading to the idea of AFM strength testing of perfect crystals. Bowden and Gane [3] had pioneered such experiments using flat ended indenters inside a scanning electron microscope (SEM). Further work on spherical indentations in materials such as {100} MgO by Macmillan and Gane [4] showed that there was a sudden plastic indentation at a high load as the tip broke through the contaminant layer which is omnipresent inside SEM chambers [5,6]. They used the Hertz theory of elastic contact to interpret their results whereas Kelly had been interested in using molecular models to derive the maximum strength using a stress criterion of failure. Experimental AFM tips are normally supplied with a nominal tip radius down to 2nm, suggesting that the atomic facet making contact could be about 4x4 atoms, so that Hertz theory of contact is not applicable. Moreover, a dynamic atomic theory of the contamination effect did not exist at that time so it was not clear whether impurities on the surface should strengthen or weaken the material.

Deleted: A

Recently there has been much interest in the molecular interpretation of AFM experiments, especially using molecular dynamics computer simulations to provide a more satisfactory theory of strength than the models given in chapter 1 of Strong Solids. For example, a flat-ended MgO probe contacting a clean MgO crystal was analysed by Yong, Smith and Kendall [7-9] and an NaCl probe

contacting an NaCl slab was described by Kendall, Yong and Smith [10] using the DL_POLY code which has been much used in atomic scale simulations [11]. The purpose of this paper is to review the AFM strength measurement using molecular simulations, then to look at the effects of probe size, shape and plasticity while finally considering the effect of contaminant layers on the crystal surfaces.

Four steps are necessary in the atomic model:

a) defining acceptable interatomic potentials,

b) adding potentials together for all the atoms in the system, assuming the total energy in the system to be built up from pairwise addition of constituent atom-atom interactions

c) calculating thermal motions of the atoms to take the dynamic nature of the system into account.

d) Working out the equilibrium condition for a range of AFM scenarios, including surface contamination.

Previous theories of solid surface interactions under water have been dominated by DLVO continuum theory (see Ref. 18) which deals with extended surfaces at relatively large separation, balancing ionic repulsions between charged double layers against the van der Waals attraction. The aim of this paper is to progress to atomistic modelling, ignoring double layer ionic effects in the first instance.

2. Model set-up; clean surfaces

The probe and slab set-up is shown in Fig 1. The slab consisted of 28x28 rows of either NaCl or MgO lattice. The Na^+–Cl^- inter-ionic spacing was 0.279 nm, while for MgO, the Mg^{2+}–O^{2-} inter-ionic spacing was 0.2104 nm. Periodic boundary conditions were applied in the x-y (horizontal) direction to mimic an infinite crystal surface with the (100) surface oriented at the z (vertical) direction. A small rectangular probe of 6 layers thick was constructed and this was varied in cross-section from the smallest possible 2x2 shown in Fig 1 to 18x18 atoms to

Deleted: DL

Deleted: molecular dynamics theory of

Deleted: an

Deleted: which is acceptable

Formatted: Indent: Left: 36 pt

Deleted: NaCl

Deleted: and the probe was 6 layers deep.

Deleted: F

Formatted: Font: Times,

Formatted: Font: Symbol

Formatted: Font: Times,

simulate increasing size of the AFM probe. Alternatively, pyramidal probes were constructed with varying contact areas from 2x2 to 10x10 atoms, These probes are small enough to ensure that they do not interact with its image neighbour in the periodic boundary conditions.

Deleted: , small enough to avoid boundary effects which caused errors with large contacts eg 15x15.

Formatted: Font color: Blue

Fig 1 Schematic of the smallest 2x2 probe approaching a crystal slab. The probe was moved towards the slab by displacing the probe rigid layer downwards, keeping the slab rigid atoms fixed. The free atoms could then find their equilibrium positions while the bath atoms maintained the temperature at 300K.

The layers of atoms were classified into three different groups as shown in Fig 1. The first three layers of atoms, labelled free, near the contacting surfaces where commensurate contact was to take place were allowed to move freely to reach their equilibrium positions. No constraint was placed on these outer layers of atoms and this ensured that the natural outcome of the atomic configurations at the surface was entirely due to the interatomic adhesion forces. However, the fourth and fifth layers of atoms were coupled to the Berendsen et al [12] heat bath to maintain the temperature of the whole system at 300K. The final layer of atoms, labelled rigid, was held fixed and gradually displaced to push the nanoprobe towards the surface. The initial gap between the surface slab and the probe was a vertical distance to the (100) surface plane, d_z, of around 1.5nm and this was gradually closed, thereby increasing the probe interaction with the slab. The surface slab and probe were orientated such that they were in commensurate contact. In each step when the probe position is updated, the whole system is allowed to equilibrate before the forces experience by the rigid probe along the z-component, F_z, is being sampled. This corresponds to an approach rate of 6. 10^{-4} ms^{-1} for equilibration before the interaction force is calculated. The whole process was repeated for different distances so that a force profile of surface interactions was obtained.

Formatted: Font: Times, Subscript

Formatted: Font: Times, Subscript

Deleted: At

Deleted: ium

Formatted: Superscript

Formatted: Superscript

Deleted: was attained at each step and

3. Results for clean surfaces

In several papers [7-9] the equilibrium was calculated for each incremental step as the contact process occurred. A still picture from the movie for NaCl just before the point of complete fracture is shown in Fig 2, but this does not reflect the true situation because all the atoms are in continuous motion. A movie is available at http://www.fuelcells.bham.ac.uk/media/nacl-md.shtml showing all the atoms vibrating around their equilibrium positions as the nanoprobe approaches and then retracts from the NaCl slab.

Deleted: www.fuelcells.bham.ac.uk

The potential chosen for this simulation contained three terms,

$$w = -e^2/r - C/r^6 + A\exp(-r/\rho) \qquad (1)$$

where e is the electron charge, r is the distance between atoms and C relates to the second-neighbour van der Waals interaction. The parameters A and ρ relate to the repulsive ionic core interactions. These constants are fitted empirically to the experimentally determined properties of NaCl such as elastic constants and crystal lattice parameters [13]. The first term is the electrostatic attraction between Na and Cl ions, the second the van der Waals attraction and the third term is the repulsion between the ions, the last two terms comprising the well-known Buckingham potential.

Deleted: spherical rigid

Fig 2 Molecular dynamics model of a sodium chloride 8x8 atom probe approaching a slab of NaCl to form new bonds with the surface atoms

For Fig 2, the potentials were added pairwise, evaluating the long-range electrostatic potentials by 3D periodic Ewald summation using the partial charge values of $\pm$ 0.988 for Na and Cl ions. Then, atomic trajectories were solved by the Verlet leapfrog algorithm with a fixed time step of 0.5fs. Initially, all moveable atoms were assigned initial velocities from a Gaussian

distribution equivalent to a temperature of 300K. The system was then allowed to equilibrate until a stable mean configurational energy was achieved, usually taking about 80 ps.

A typical force versus distance curve for the 8x8 NaCl probe is given in Fig 3. The probe movement started on the right as shown by the bold line and it was clear that there was near zero force of attraction at this stage. The probe was then moved towards the slab until an attractive force was experienced.

Fig 3 Force per ion versus distance curves for approach from right to left and withdrawal of the 8x8 NaCl nanoprobe showing the jump to contact and the equilibrium at zero force

Then a sharp change in F_z was observed, the 'jump to contact'. Further displacement caused the force to approach zero, the equilibrium contact position. Subsequently, the probe was compressed as it was pushed into the slab giving elastic indentation to the left of Fig 3. The withdrawal was essentially reversible but the 'jump from contact' or fracture of the bond was slightly delayed, indicating cohesion hysteresis, although the strength was essentially the same. This indicates that strength should be calculated equally on both make and break of the bonds. By changing the size of the nanoprobe, the average work of cohesion W in joules per square metre could be calculated from the model and compared with the breaking stress (ie pull-off force /contact area) in GPa as shown in Table 1.

Table 1 Work of cohesion W and average breaking stress for the different size NaCl probes

Contact size	**area/nm^2**	**W/ Jm^{-2}**	**stress/GPa**
(2 × 2)	0.3114	0.47	4.03
(4 × 4)	1.2455	0.48	3.06
(6 × 6)	2.8023	0.44	2.55

Deleted: i

Deleted:

Deleted:

Deleted: article

Deleted: the particle

(8 × 8)	4.9818	0.45	2.42
(10 × 10)	7.7841	0.45	2.38
(14 × 14)	15.257	0.44	2.08
(18 × 18)	25.220	0.43	2.03

It can be seen that the work of cohesion remained almost constant, as assumed in the continuum theory of fracture [14] but the stress decreased as the AFM probe got bigger as expected from fracture mechanics theory. In other words, the stress criterion of fracture assumed by Kelly does not apply in this model. In addition, it may be seen that the energy is dominated by the electrostatic forces for NaCl; a van der Waals probe contact would have W around $0.1 Jm^{-2}$. The maximum strength was calculated to be 4.03 GPa compared to 2.4 GPa calculated in the book Strong Solids.

Deleted: particle

4. Elastic and plastic deformation

The 8x8 rectangular NaCl nanoprobe behaved elastically and separated cleanly despite the large attractive interatomic forces. More commonly, for MgO and also for pyramidal probes, the forces rose so high as the separation occurred that the atoms were displaced from their normal positions and irreversible plastic deformation took place. Fig 4 shows the computed results for a stepped NaCl nanoprobe of contact size 8x8 in contrast to a stepped probe with contact size of 4x4. As stress was applied to the 8x8 contact (Fig 4 top), separation did not occur, but the step acted as a defect which promoted plastic deformation, allowing the NaCl crystal probe to extend in line with the applied force. The smaller contact (Fig 4 bottom) also began to deform plastically, but separation then took place at the interface such that the nanoprobe was released but extra energy was expended in creating a plastic defect hole in the probe. This model shows that there should be an elastic/plastic transition for larger nanoprobes, such that material transfer from the probe to the slab occurred. By modelling

Deleted: article
Deleted: article
Deleted: article
Deleted: particle
Deleted: particles

increased contact sizes of NaCl pyramidal probes [8], it was shown that small contacts eg 2x2 were brittle but larger contacts eg 8x8 became plastic as the nanoprobe was pulled off.

Plastic deformation could also be induced by preloading the probe in compression such that plastic collapse occurred at high force. This introduced defects into the probe, causing subsequent plastic flow when the probe was withdrawn [8].

Fig 4 (top) Major plastic deformation observed in the 8x8 contact model of the pyramidal NaCl nanoprobe.
(bottom) Results for 4x4 NaCl contact show clean detachment with minor plastic deformation

Deleted: particle

Formatted: Bullets and Numbering

5. Influence of plastic flow on strength

The influence of the plastic flow on the observed strength measurement could be studied by comparing the reversibility of the force curves during jump to contact then pull-off. Fig 5 shows the force distance curves computed for the pyramidal NaCl probe shown in Fig 4 (bottom). The jump to contact during approach caused no damage to the lattice structure and the strength calculated by dividing the total z-component force in the base of the probe by the area of the contact was 3.6 GPa. This was somewhat higher for the pyramidal probe than that calculated for a flat 4x4 NaCl probe seen in Table 1 which gave a strength of 3.1 GPa.

Deleted: per ion

Deleted: ion

Deleted: from the result

Deleted:

Fig 5 Force per ion in 10x10 rigid layer vs displacement curve for pyramidal 4x4 NaCl probe. The jump to contact appears perfectly elastic but the pull-off dissipates energy without raising the force significantly. The stress required for compressive collapse was much higher.

Deleted: Force per ion vs displacement curve for pyramidal 4x4 NaCl probe. The jump to contact appears perfectly elastic but the pull-off dissipates energy without raising the force significantly. The stress required for compressive collapse was much higher.

The most significant observation from Fig 5 was that the compressive collapse strength of the NaCl probe, 19.3 GPa, was very much higher than the tensile strength of 3.6 GPa. This is more like a hardness measurement in which plastic flow is required to produce an indentation, typically requiring three times more pressure that tensile yielding.

MgO showed very similar behaviour but at higher stresses and with more plastic deformation during pull-off. The 6x6 pyramidal MgO probe gave a jump-to-contact strength of 14.4 GPa without any lattice damage. On pull-off, the same stress was observed, demonstrating reversibility. But then substantial plastic deformation occurred and the jump-from-contact occurred in a series of steps with large dissipation (Fig 6) indicating increased toughness.

Fig 6 Force vs displacement curve for 6x6 pyramidal MgO probe showing that the jump to contact was perfectly elastic. The pull-off was at the same force but dissipated energy plastically. The steps in the breaking curve were due to sudden motion of defects within the nanoprobe, which remained attached to the slab.

Compression of the probe into the slab eventually caused plastic collapse at a stress of 65 GPa, showing that the compressive strength was about five times higher than the tensile strength.

In conclusion, it is evident that a number of complex processes can influence nanoprobe strength including the nature of the crystalline material, the atomic contact, its loading history, the shape of the probe, tension or compression and the propensity for plastic flow.

Deleted: of

Formatted: Bullets and Numbering

6. Influence of surface contamination

The cohesive forces for clean NaCl surfaces were seen to be very large, leading to plastic effects and irreversibility, with adhesive energies around 0.47 Jm^{-2}. Of course, this can only be true for atomically clean surfaces, as tested in high vacuum experiments with baked out materials. In practical AFM testing, ubiquitous contamination such as nitrogen or water adsorbs on the surface and this has a very large effect of reducing the adhesive energy to much smaller values around 0.1 Jm^{-2} or even lower if thicker layers of contamination build up leading to energy and force oscillations first proposed by Kendall [15]. For example, Fig 7 shows a computational model of a pyramidal 6x6 MgO probe pushed towards an MgO slab

Deleted: force

Deleted: -

Formatted: Superscript

Deleted: nN

whose surface was covered by inert gas particle spheres with xenon-like van der Waals attributes at 100K.

Deleted: (xenon-like) molecules

Fig 7 a),b) Stills from a movie of molecular dynamics model of 6x6 MgO pyramidal probe approaching an MgO slab coated with a monolayer of xenon molecules at 100K; c)force distance curve approaching from right to left, showing steps as molecules are squeezed out.

The 6×6 MgO probe was surrounded by the Lennard Jones (LJ) xenon-like spheres and it was immediately evident that these xenon molecules formed structured layers around the probe and upon the slab surface, with 3 distinct layers easily visible (Fig 7 a & b). Each sphere was weakly interacting with the surface atoms with an energy parameter of $\varepsilon = 0.02$ eV and $\sigma = 0.305$ nm at a temperature of 100 K. Fig. 7c shows the response of the MgO probe in the presence of the contaminant, with the contact force increasing from right to left as the gap was squeezed. The contamination prevented the jump-to-contact in this case but there were four significant steps; first at 0.02nN where a slight bump could be seen, second at 0.1 nN as the third layer of xenon was penetrated at 3.5nm; next at 0.35 nN as the second xenon layer was squeezed out at 3.2nm; and finally at 0.9 nN as the probe collapsed plastically at high force because the first xenon layer could not be squeezed out by the probe.

Deleted: 5

Deleted: 3.9c

Similar calculations had been carried out previously by Gao et al [16] but their probe shown in Fig 8 had not been suitable for experimental study because of its infinite length. However, they did show that the structuring phenomenon was moderated by the alignment of the solid surfaces, with commensurate crystals showing strong liquid structuring in the model.

Deleted: geometry

Deleted: 6

Fig 8 Molecular dynamics model of Gao et al [16] showing the flat parallel plate configuration with liquid in between; the solid surfaces were infinite in the y direction.

That simulation had shown squeezing out of the contaminant molecules in discrete steps, rather like the experimental results found in mica experiments by Horn, Pashley et al [17-19]. AFM experiments have not found this effect consistently, although Lim et al [20] showed stepwise squeezing out of organic molecules such as n-dodecanol from a graphite substrate, depending strongly on the size of the AFM tip, with finer tips (R_{tip}=25nm) giving reliable force measurement. They detected about 6 layers of molecules squeezing step-wise from the graphite, and also suggested the full tip contact with the graphite could be obtained using Si_3N_4 AFM probes. Most previous experiments on this effect with water have been carried out with mica surfaces in the presence of ions [21] and this has been modelled by Leng [22] to show the repulsions associated with structured water layers. The purpose of our study was to use an AFM geometry to test the strength of MgO in the presence of water.

Formatted: Bullets and Numbering

7. Simulation of water between MgO surfaces

To investigate the question of how water could be squeezed out from oxide surfaces in AFM strength testing, the model illustrated in Fig 9 was set up. The baseline comparison was with clean MgO which gave the results shown in Fig 6. The calculations for clean MgO were compared to the model with 3 layers of water molecules positioned on the slab as the probe was moved downwards (Fig 9a). The potential for water interacting with MgO was derived from de Leeuw and Parker [23]. The calculations showed that the jump to contact forces (Fig 9b) were much reduced by the presence of the water molecules. As the probe moved towards the slab, some water molecules jumped across the gap to cover the probe surface in a monolayer, causing a dip in the approach force curve as the gap between the MgO surfaces was fully filled with water. Then one layer of water was squeezed out as shown by the increase in force followed by a drop. Two more layers were then squeezed out at increasing force, but the final layer could not be removed in this model. On withdrawal, the force curves were not reversible but showed some hysteresis as the water penetrated back into the gap between probe and slab. It was clear that the MgO probe could now be removed from the MgO slab without any plastic deformation, which was impossible for the clean

Deleted: a

Deleted: 10

surfaces. The maximum tensile stress at pull-off was 1.57 GPa compared to 14.4 GPa for clean surfaces, illustrating the factor of nine weakening effect of water in tension.

Fig 9a) Pyramidal 6x6 MgO probe moving towards an MgO slab covered with 3 layers of water molecules; b) force distance curve revealing the filling of the gap then the oscillations as three layers of water were squeezed out, leaving one layer resisting removal, showing hysteresis

A key question was whether the strength of the MgO was increased by the surface contaminant, as suggested in Strong Solids. To test this, the force on the probe was increased until the MgO collapsed plastically. With water present, the collapse stress for the 6x6 MgO probe was 9.6 GPa compared to 65 GPa for the clean probe, showing that the contamination had given a factor of seven weakening in compression.

Deleted: as shown in Fig 9a

Deleted:

One of the most interesting features of this model is that there are now several zeros in the force versus separation curve, depending on the number of water molecule layers separating the surfaces, intimating that the probe could appear to be in equilibrium at several separation values depending on the applied force. There were three discrete equilibria at gaps of 0.5 nm, 0.75 nm and 1nm. This raises the question of colloidal stability of MgO particles in water, where the kT of thermal energy of the particles will push the contacts into one of the energy wells by squeezing out one or more water layers [24].

Conclusions

Strength of perfect crystals can be measured in the Atomic Force Microscope if the theory of crystal fracture and plasticity is understood. Molecular dynamics models of NaCl and MgO probes pushed into perfect crystal substrates have been used to interpret the processes at the nanometer level for comparison with AFM tests.

Clean surfaces of NaCl or MgO attract each other and pyramidal probes give the expected 'jump to contact' followed by continued approach to equilibrium at zero force. This process was found to be

elastic and reversible with NaCl flat probes, showing that the nanocrystals could be pulled apart without damage and that the strength of 4.03 GPa was reversible, ie equal on approach and pull-off, though slight 'cohesion hysteresis' was observed. NaCl followed an energy criterion of fracture in this case, showing essentially brittle fracture, with strength diminishing for larger probes as expected from fracture mechanics.

Plastic flow of the NaCl probes could be encouraged by several means:- first by enlarging the contact region, second by changing the probe shape and thirdly by damaging the probe. MgO showed the same effects but differed from NaCl in that plastic flow always dominated the behaviour. Another measure of MgO strength was the probe collapse which was observed when increased compression of the probe onto the slab were made. Plastic collapse of the probe took place at a well defined compressive stress of 65 GPa, larger than the tensile strength of 14.4 GPa measured at jump to contact and pull-off.

Deleted: computations of

When the MgO surfaces were contaminated with water molecules, there was a very significant change in behaviour. First, the jump to contact was now periodic as layers of molecules were squeezed out from the gap between probe and slab. Second, the process of detachment was now easier and the MgO probe could be detached at low tensile stress of 1.57 GPa without damage. Third, the strength of the MgO probe as it collapsed on severe compression into the slab was altered. The compressive strength was diminished by a factor 7 in the presence of the water molecules.

References

1. A. Kelly and N.H. Macmillan, *Strong Solids*, 3rd Edition, Clarendon Press Oxford 1986, pp.47-50; A. Kelly, *Strong Solids*, 1st edition, Clarendon, Oxford 1966.
2. F. Zwicky, Phys Zeit 24(1923)p.131

3. N. Gane and F.P. Bowden, J Appl Phys 39(1968) p.1432.
4. N.H. Macmillan and N. Gane, J Appl Phys 41 (1970)p.672.
5. N. Gane, Proc R Soc Lond A317((1970)p.367.
6. J.B. Pethica and D. Tabor, Surf Sci 89 (1979) p.182.
7. C.W. Yong, W. Smith and K. Kendall, J Mater Chem 12(2002)p.593.
8. C.W. Yong, W. Smith, A.Dhir and K. Kendall, Tribology Letters 26(2007)p.235.
9. C.W.Yong, K. Kendall and W. Smith, Phil Trans R Soc Lond A362(2004)p.1915.
10. K. Kendall, C.W. Yong and W. Smith, J Adhesion 81(2004)p. 21.
11. W. Smith and T. Forrester, DL_POLY, version 2.12 (CCLRC,Daresbury Laboratory, UK, 2001; Smith, W., (ed) *Molecular Simulation*, 32(2006) **p.**933.
12. H.J.C. Berendsen, J.P.M. Postma, W.F.van Gunsteren, A. DiNola, andJ.R. Haak, J Chem Phys 81(1984)p.3684.
13. C.R.A. Catlow, K.M. Diller and M.J. Norgett, J. Phys. C 10(1977) p.1395.
14. K. Kendall, *Molecular adhesion and its applications*, Kluwer Academic, New York 2001
15. K.Kendall, J Adhesion 5(1973)p.179.
16. J. Gao, W.D. Luedtke and U. Landman, Phys Rev Lett 79(1997) p.705.
17. R.G.Horn and J.N. Israelachvili, J Chem Phys **75**(1981) p.1400.
18. J.N. Israelachvili, *Intermolecular and Surface Forces*, Academic Press, London 1985,pp.198-201.
19. R.M. Pashley and J.N. Israelachvili, J Colloid Interface Sci 101(1984) p.511.
20. L.T.W. Lim, A.T.S. Wee and S.J. Oshea, Langmuir 24(2008) p.2277.
21. D. Gourdon and J.N. Israelachvili, Phys Rev Lett 96(2006)099601.
22. Y. Leng,Y., J Phys Condens Matter 20(2008)354017.
23. N.H. de Leeuw and S.C. Parker, Phys. Rev. B 58 (1998)p.13901.
24. K. Kendall, A. Dhir and S. Du, Nanotechnology 20(2009)275701 (4pp)

Deleted: Nanotechnology 14(2003)p.829

Deleted: , K.

Deleted: Dhir, A., Yong, C.W., and

Deleted: , K.

Figs for '**Strength by Atomic Force Microscopy (AFM): Molecular dynamics of water layer squeezing on magnesium oxide'** by K. Kendall, A. Dhir & C.W. Yong

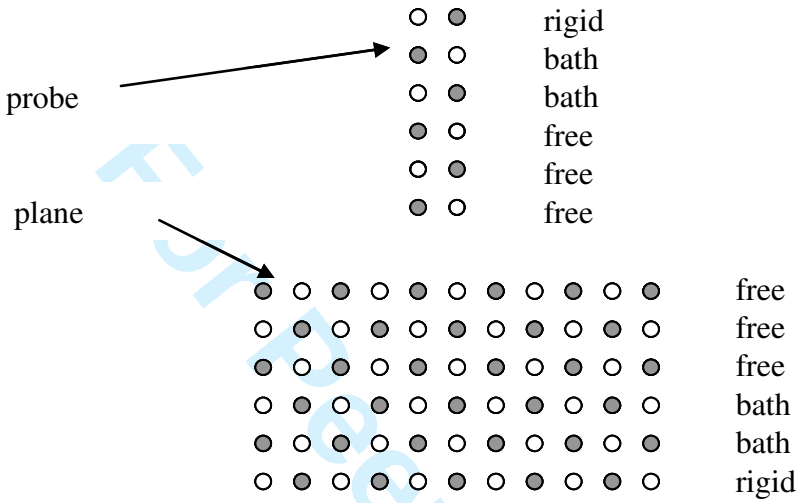

Fig 1 Schematic of the smallest 2x2 probe approaching a crystal slab. The probe was moved towards the slab by displacing the probe rigid layer downwards, keeping the slab rigid atoms fixed. The free atoms could then find their equilibrium positions while the bath atoms maintained the temperature at 300K.

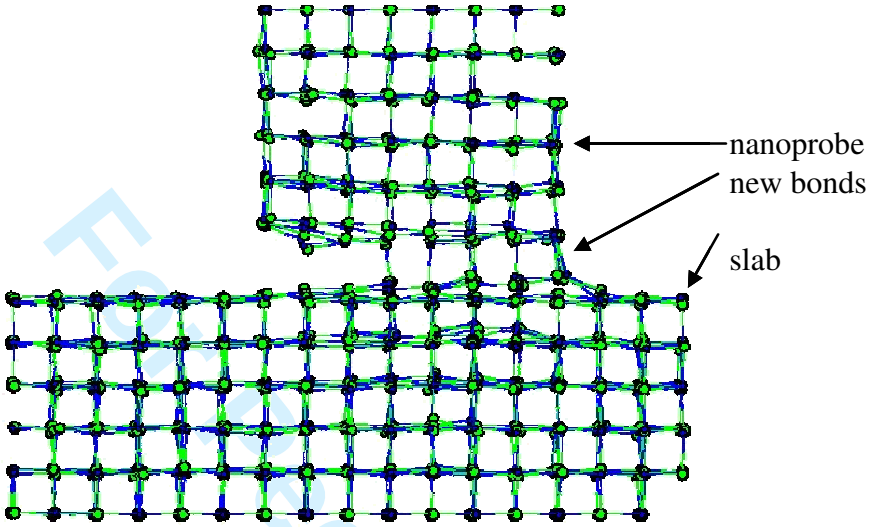

Fig 2 Molecular dynamics model of a sodium chloride 8x8 atom probe approaching a slab of NaCl to form new bonds with the surface atoms

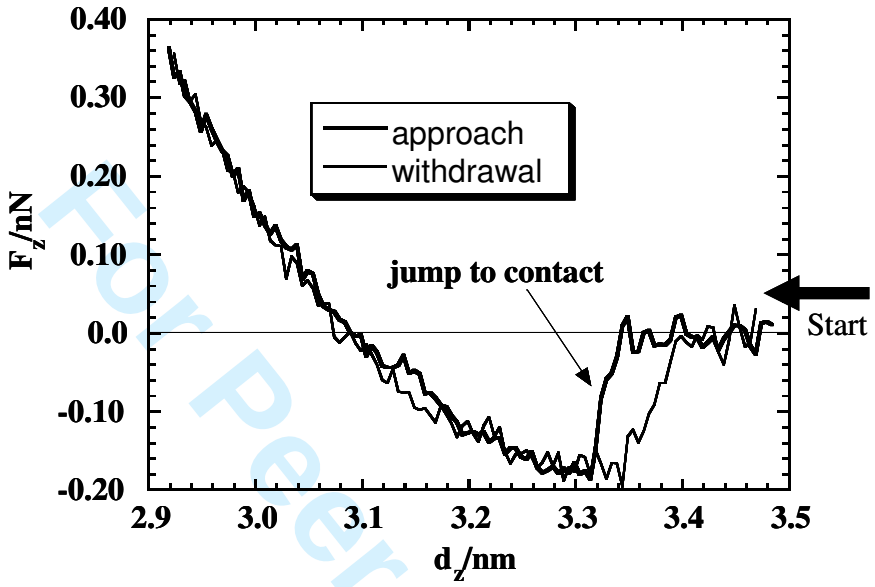

Fig 3 Force per ion versus distance curves for approach from right to left and withdrawal of the 8x8 NaCl nanoprobe showing the jump to contact and the equilibrium at zero force

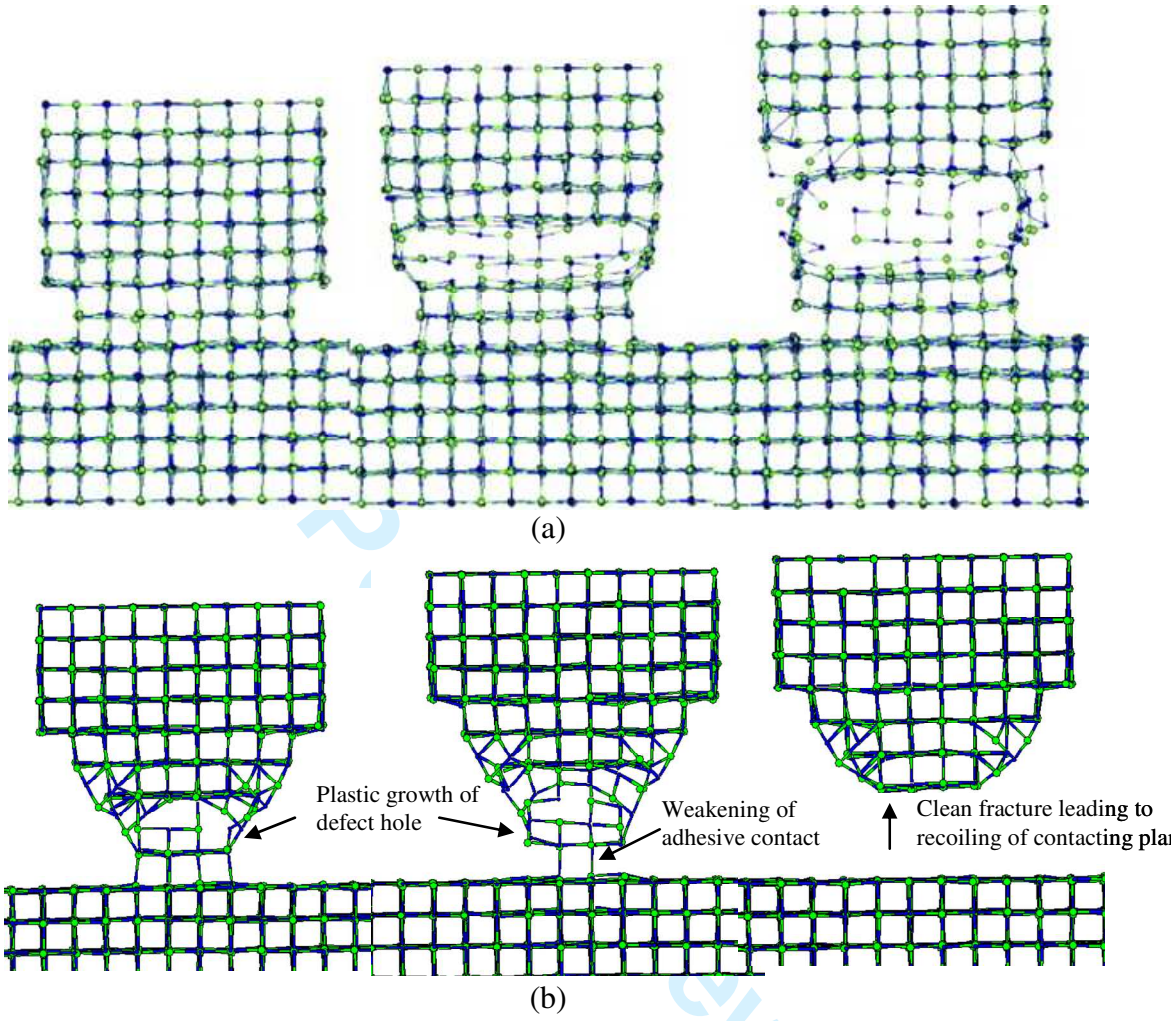

Fig 4 (a) Major plastic deformation observed in the 8x8 contact model of the pyramidal NaCl nanoparticle. (b) Computed results for 4x4 NaCl contact show clean detachment with minor plastic deformation

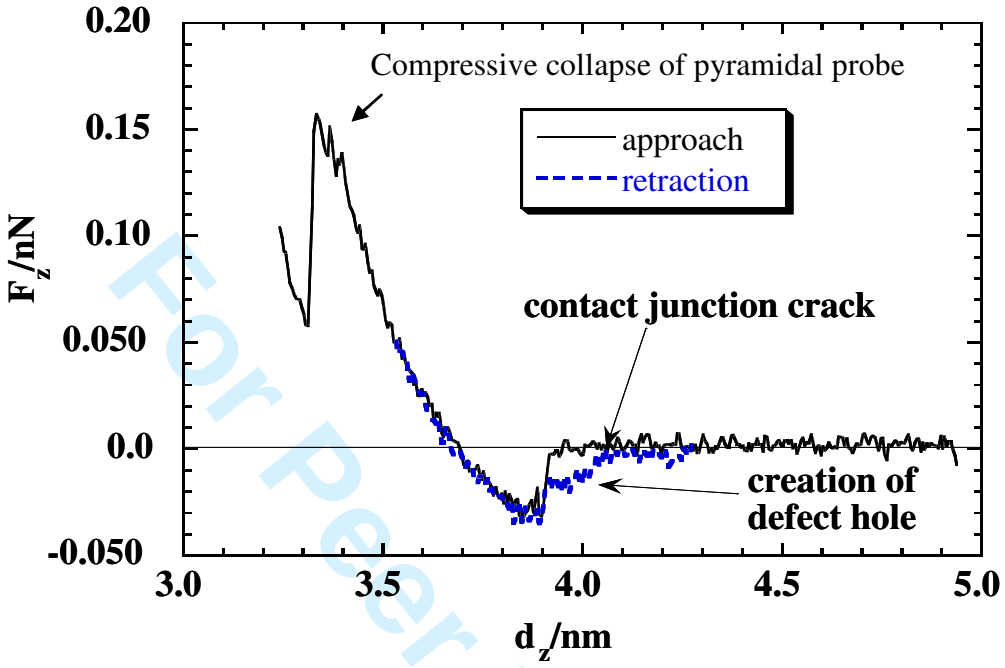

Fig 5 Force per ion in 10x10 rigid layer vs displacement curve for pyramidal 4x4 NaCl probe. The jump to contact appears perfectly elastic but the pull-off dissipates energy without raising the force significantly. The stress required for compressive collapse was much higher.

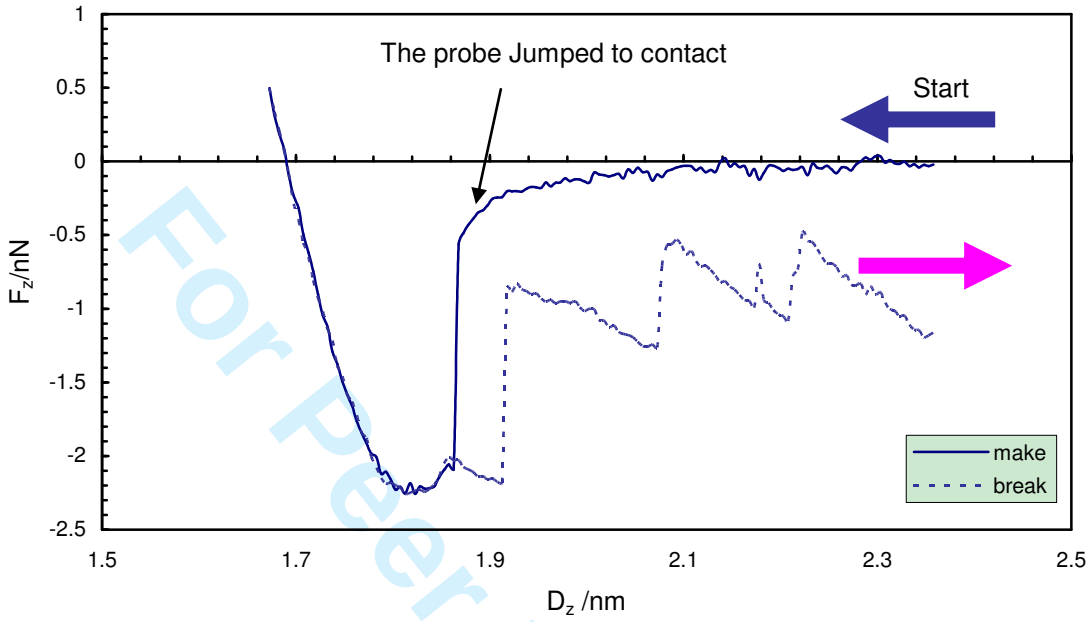

Fig 6 Force per 10x10 ion vs displacement curve for 6x6 pyramidal MgO probe showing that the jump to contact was perfectly elastic. The pull-off was at the same force but dissipated energy plastically. The steps in the breaking curve were due to sudden motion of defects within the nanoprobe, which remained attached to the slab.

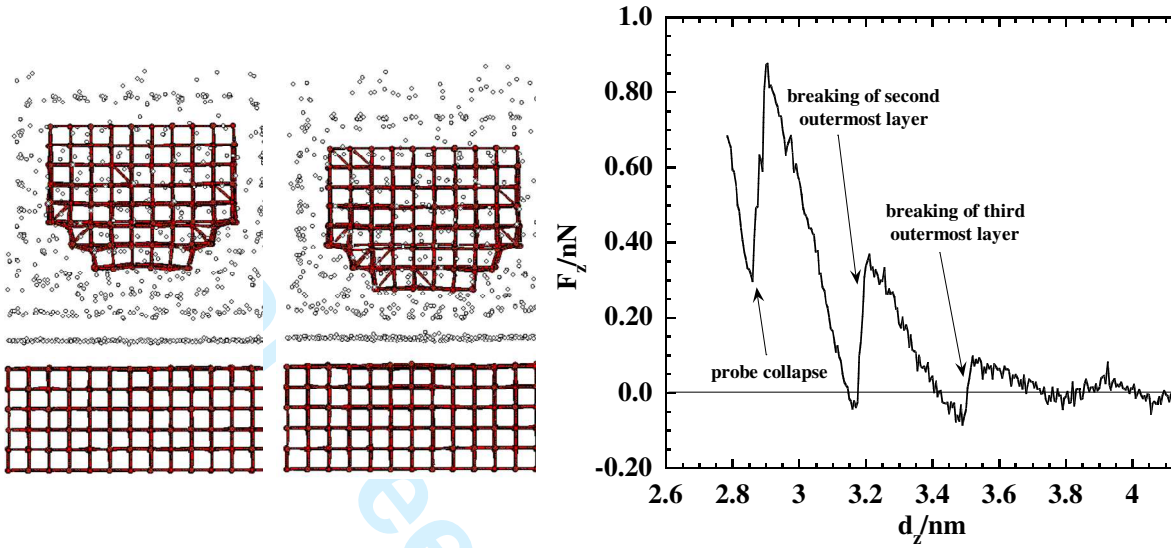

(a) (b) (c)

Fig 7 a),b) Stills from a movie of molecular dynamics model of 6x6 MgO pyramidal probe approaching an MgO slab coated with a monolayer of xenon molecules at 100K; c)force distance curve approaching from right to left, showing steps as molecules are squeezed out.

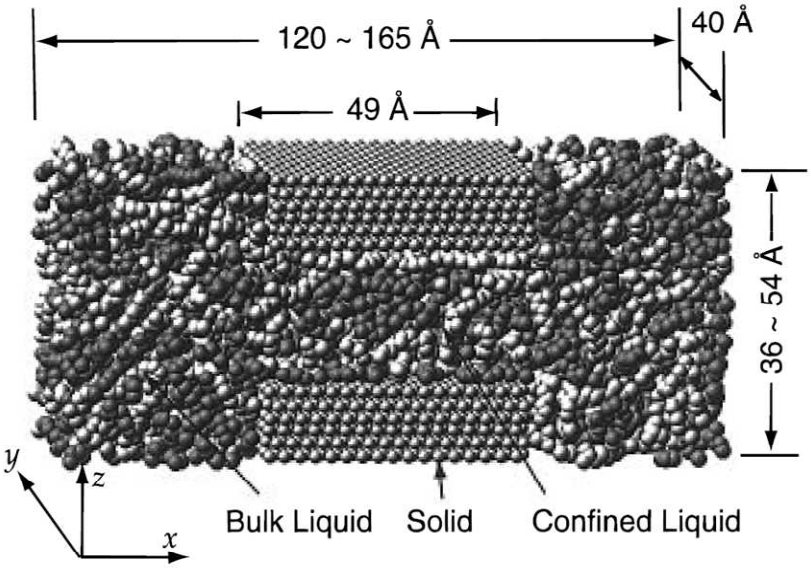

Fig 8 Molecular dynamics model of Gao et al (1997) showing the flat parallel plate configuration with liquid in between; the solid surfaces were infinite in the y direction.

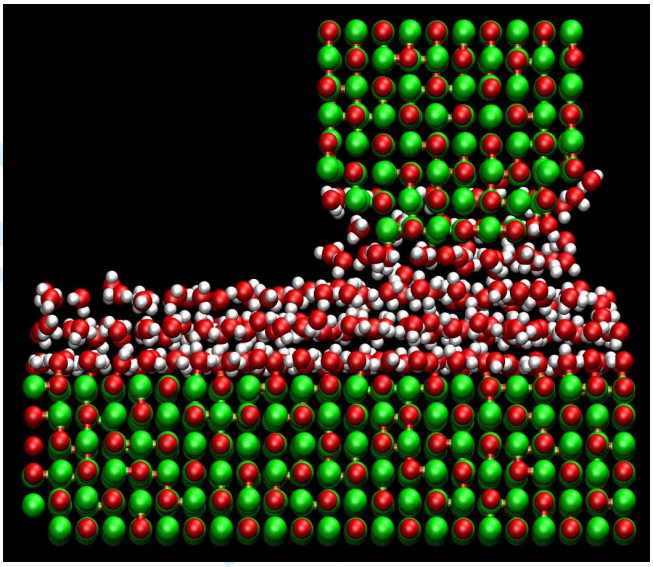

(a)

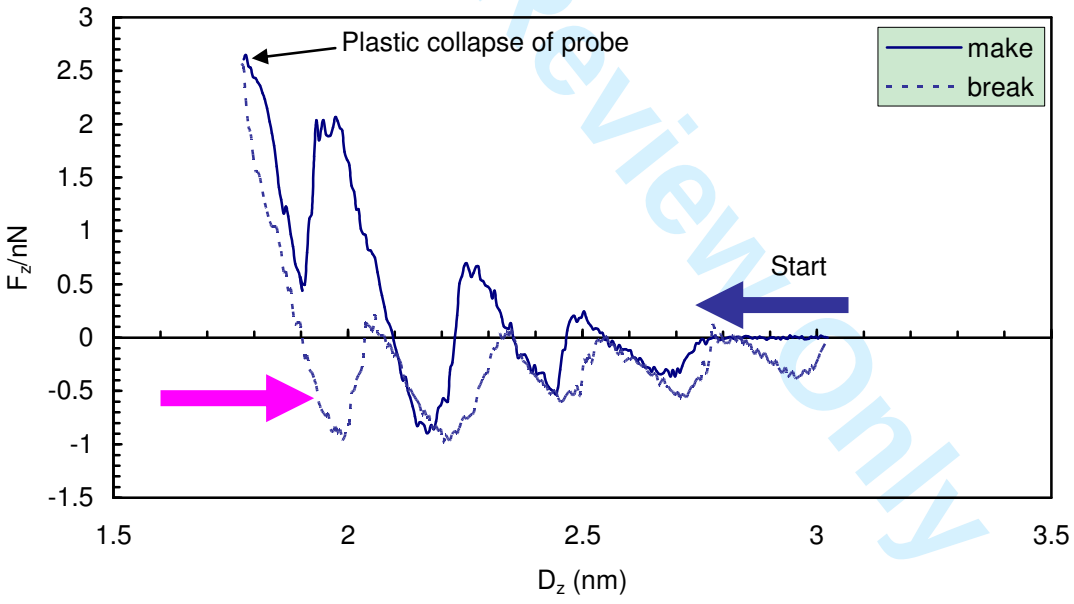

(b)

Fig 9a) Pyramidal 6x6 MgO probe moving towards an MgO slab covered with 3 layers of water molecules; b) force distance curve revealing the filling of the gap then the oscillations as three layers of water were squeezed out, leaving one layer resisting removal, showing hysteresis